COMMUNICATION

Soft Transfer Printing of Chemically Converted Graphene

By *Matthew J. Allen, Vincent C. Tung, Lewis Gomez, Zheng Xu, Li-Min Chen, Kurt S. Nelson, Chongwu Zhou, Richard B. Kaner,* and *Yang Yang**

Since its experimental discovery in 2003, there has been great interest in single layer graphene for a variety of applications. Ballistic transport of electrons along the atomically thin layer, along with mobilities exceeding 15 000 $cm^2 V^{-1} s^{-1}$ and an ambipolar field effect make graphene a particularly good candidate for the next round of semiconductor devices.[1–6]

Although similarities to carbon nanotubes and other conjugated systems help contribute to the theoretical understanding of graphene, experimental results have been less forthcoming due to the difficulty in producing single layer specimens. As with carbon nanotubes, the large aspect ratio of individual sheets, and strong van der Waals forces holding them together, make isolating single sheets of graphene very challenging.

Thus far only two methods have enjoyed reliable success; the Scotch tape or "drawing" method and by the reduction of silicon carbide.[6] The drawing method utilizes a piece of cellophane tape to draw a thin film from highly oriented pyrolytic graphite (HOPG). After repeated peeling from the thin film, it is ultimately stamped onto a substrate and the tape is carefully removed. The resulting deposition is a dense network of both single and multi-layered graphene, which must be scoured using an optical microscope and otherwise characterized before finally a single sheet may be reliably identified for further use. Alternatively, the reduction of silicon carbide (SiC) reliably produces small regions of graphitized carbon, but requires temperatures greater than 1000 °C.[7,8]

While these methods have provided adequate samples for preliminary experimental results, both present a number of drawbacks and neither is well suited for industrial applications. First and foremost, the yield of single sheets produced is exceedingly low. Furthermore, the location of those specimens is largely random, and certainly not controllable to the level required for mass fabrication techniques. Finally, neither the peeling method nor the reduction of silicon carbide is scalable or high-throughput. These necessary conditions for the ultimate goal of graphene electronics present formidable hurdles and will continue to motivate research.

Chemists have recently proposed a third synthetic route through the oxidation and exfoliation of graphite, which may provide a number of advantages.[9–13] The resulting single sheets of oxidized graphite are stable as uniform aqueous dispersions. Although graphite oxide is itself an insulator, the sheets may be restored to semi-metallic graphene, and its planar structure, by chemical reduction or by thermal annealing. The technique has led to a number of functioning single sheet field-effect

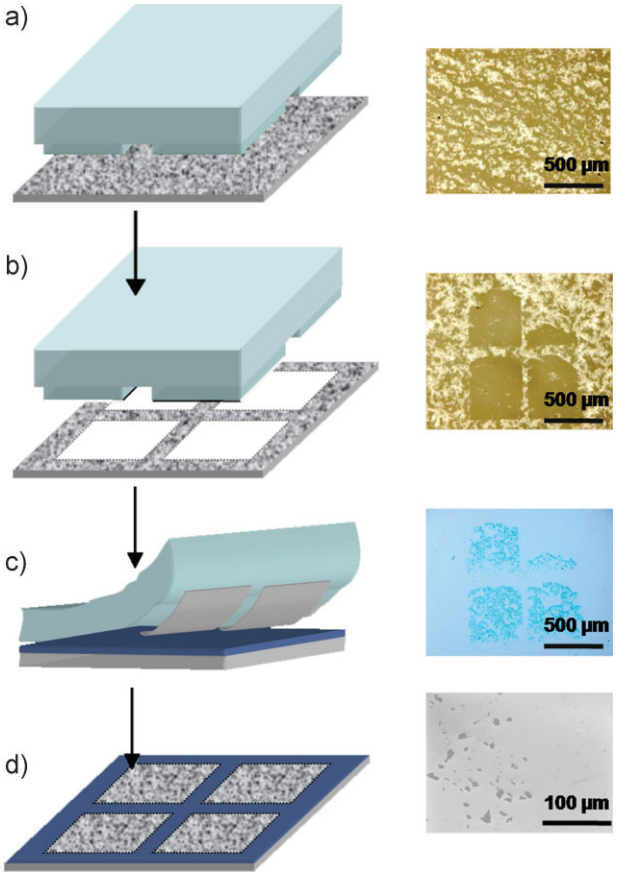

Figure 1. A diagram (left) and optical microscope images (right) depict the PDMS transfer process. It begins by a) depositing materials on a glass substrate and b) carefully "inking" the pre-patterned PDMS stamp. c) The inked stamp is contacted to a heated Si/SiO_2 substrate and d) peeled away to reveal deposited materials.

[*] Prof. Y. Yang, V. C. Tung, Z. Xu, L.-M. Chen, Prof. R. B. Kaner
Department of Materials Science and Engineering and
California NanoSystem Instute
University of California, Los Angeles
Los Angeles, CA 90095 (USA)
E-mail: yangy@ucla.edu
M. J. Allen, K. S. Nelson, Prof. R. B. Kaner
Department of Chemistry and Biochemistry and
California NanoSystems Institute
University of California Los Angeles, Los Angeles, CA 90095 (USA)
L. Gomez, Prof. C. Zhou
Department of Electrical Engineering, University of
Southern California
Los Angeles, CA 90089 (USA)

DOI: 10.1002/adma.200803000

devices.[14,15] Fabrication typically includes air-brushing or spin-coating from water, followed by an electron-beam process to deposit electrodes, and chemical reduction. Although graphite oxide dispersions facilitate some solution processing, the location of single sheets has been uncontrollable and individual sheets often aggregate due to the high surface tension of water.[11]

In this work, graphite oxide was isolated and subsequently dispersed directly in anhydrous hydrazine. The method utilizes hydrazine both as a reducing agent and as a dispersent. Suspensions in hydrazine have been shown to preserve the integrity of large sheets and tend not to aggregate.[16] After modification by dilution, centrifugation, or ultrasonication, we were able to obtain a variety of controllable surface coverages (see Supporting Information). Prepared depositions were quite uniform, and allowed for a range of both coverage densities and sheet sizes. Subsequent to deposition, a transfer printing process enabled us to selectively register regions of graphene to designated areas of another substrate. The non-destructive printing process is capable of defining small features and transferring depositions to precise positions.[17–21] Although transfer printing of graphene has been previously reported using hard stamps to cut and exfoliate small areas from HOPG,[22,23] this report presents soft stamping after the large-scale deposition of chemically converted graphene from solution. Although soft stamps are less durable and capable of lower feature resolution than hard ones, they enjoy the advantages of mechanical flexibility, versatility and ease of fabrication.

Transfer Printing: The transfer mechanism utilized here is based on the differing strengths of non-covalent adhesion at the PDMS-graphene and graphene-substrate interfaces. For most materials, the PDMS interface is weaker than the substrate interface, due to the extremely low surface energy of PDMS (19.8 mJ m^{-2}).[24] Transferring of graphitic specimens by a PDMS stamp is depicted in Figure 1. The process begins by spin-coating hydrazine suspensions onto an oxygen plasma treated glass substrate, followed by a thermal annealing process to remove solvent and hydrazinium cations.[16] Spin speed and the composition of hydrazine suspensions essentially determine the density of flakes in deposited films, which can be varied from thicker overlapping coatings (≈3 nm) to those of evenly spaced single sheets (see Supporting Information). An optical image of a dense deposition, which provides good optical contrast on glass, is provided on the right-hand side of Figure 1a.

Glass substrates were brought into contact with a patterned PDMS stamp as shown in Figure 1b. In this case, the stamp was designed with four raised rectangles. The weight of a coin (U.S. penny) was used to ensure intimate contact, and was left in place for 2 minutes for complete transfer. The hydrophobic surface of pristine PDMS interacts more strongly with graphene than does the initial glass substrate, which allows transfer to take place. Graphene registered PDMS stamps were then peeled from the glass substrate. An optical image after peeling clearly shows that material was completely removed in three of the four rectangular areas of contact (Fig. 1b, right). The fourth pad shows only partial removal, which we commonly observe and attribute to an uneven height profile, or low spots, of the stamp. In this step, freshly prepared PDMS provided much greater yield than older

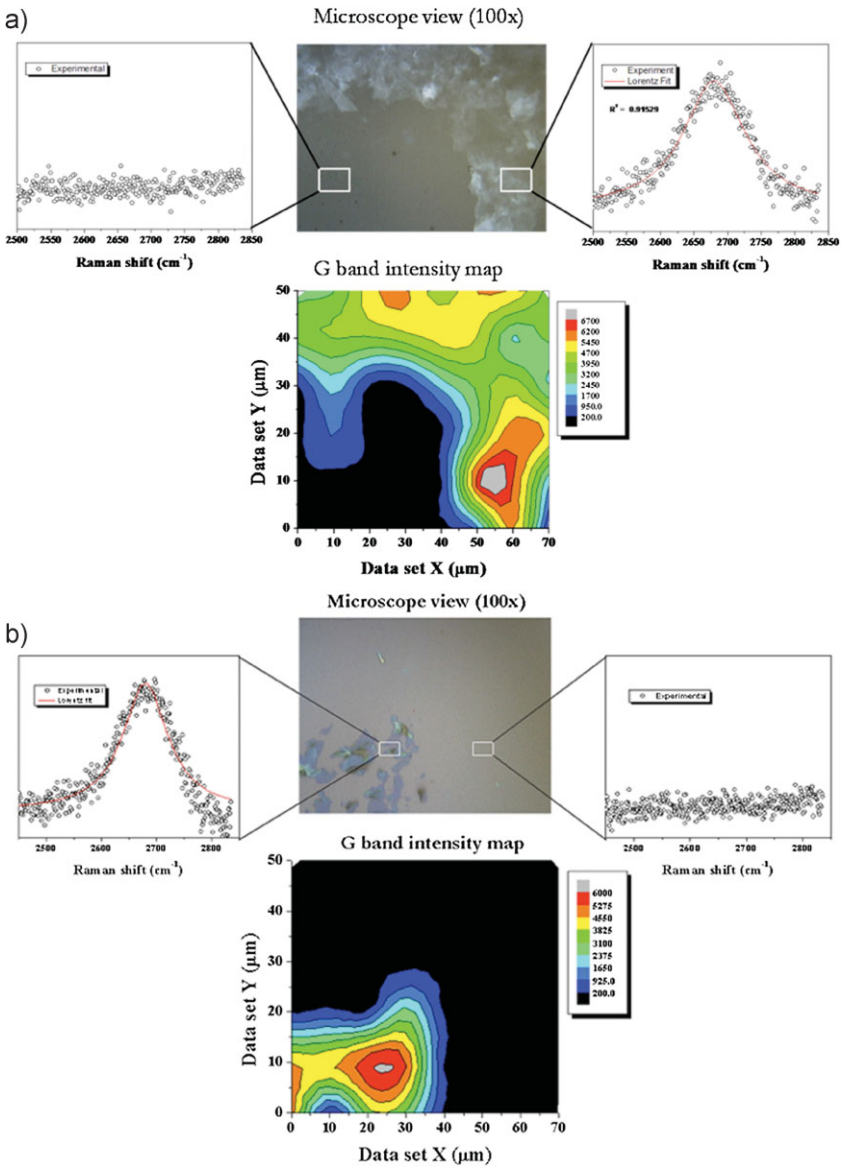

Figure 2. Micro-Raman spectra were collected inside and outside a rectangular region on a) glass and b) Si/SiO_2. Raman intensity mapping of the *G* peak indicates that graphene has been removed completely from a section of the glass by the PDMS stamp and successfully deposited onto a Si/SiO_2 substrate. Representative spectra are provided for spots both inside and outside of the rectangular regions showing the *G′* peak of graphitic carbon.

stamps, which had undergone significant cross-linking and hardening when left under ambient conditions.

"Inked" stamps were next carefully brought into contact with 300 nm Si/SiO_2 substrates (Fig. 1c). Contact time of several days was necessary to fully transfer single sheets from PDMS to Si/SiO_2 substrates at room temperature. Transfer proceeded as low molecular weight oligomers were dissociated from the surface of the stamp over time, releasing the graphene sheets.[25,26] With the assistance of heat, oligomers were more quickly dissociated from the PDMS stamp, allowing full transfer in 2 h at 50 °C and 30 min at 75 °C. Heating also facilitated reorientation and segmental motion, which further weakened the interface between graphene and PDMS. The stamp was finally removed from the Si/SiO_2 substrate, leaving behind the rectangular pattern of graphene as shown in bright-field (Fig. 1c, right) microscope images. The same methods were applicable no matter the density of parent depositions. The neat edge of a separate transferred film comprised of sparse single sheets is shown in the SEM image of Figure 1d, right. Insufficient temperature or contact time both resulted in only partial transfer, with residual flakes remaining on the stamp after removal.

Characterization of Transfer. Although the initial characterization of a deposition was carried out optically, more sophisticated techniques were necessary to understand the extent to which transfer had taken place. Figure 2 presents optical images and the corresponding *G* band Raman intensity maps of both the glass (a) and Si/SiO_2 (b) substrates used during the transfer process. The *G* band at 1584 cm^{-1} results from the E_{2g} vibrational mode in graphene and is not observed on a clean Si/SiO_2 surface.[27–31] A *G* band intensity map for the glass substrate (Fig. 2a) clearly shows that graphitic materials have been almost completely removed from the rectangular region that contacted the PDMS stamp. The removed region has well defined borders, including a nearly right angle at the upper right-hand side. A *G* band intensity map for the Si/SiO_2 substrate (Fig. 2b) indicates a well-defined rectangular region of transferred graphitic material, closely resembling the PDMS stamp features.

Removal of PDMS Residue: Although they were not visible in the Raman spectra, our understanding of the PDMS transfer process suggested that there were likely dimethylsiloxane oligomers deposited along with graphene. This is often the case with transfer printing and can represent a problem for subsequent fabrication techniques.[25,26] In order to remove oligomers, we thermally annealed the deposited material at 400 °C for 1 hour in the vacuum of an XPS chamber. Figure 3 shows C 1s (a,b) and Si 2p (c,d) XPS spectra from the deposited region both before and after annealing. The Si peak is predominately Si/SiO_2, but displays a large shoulder consistent with dimethylsiloxane before the annealing process. The shoulder was nearly gone after heating at 100 °C and entirely removed after annealing at 400 °C for 1 hour,

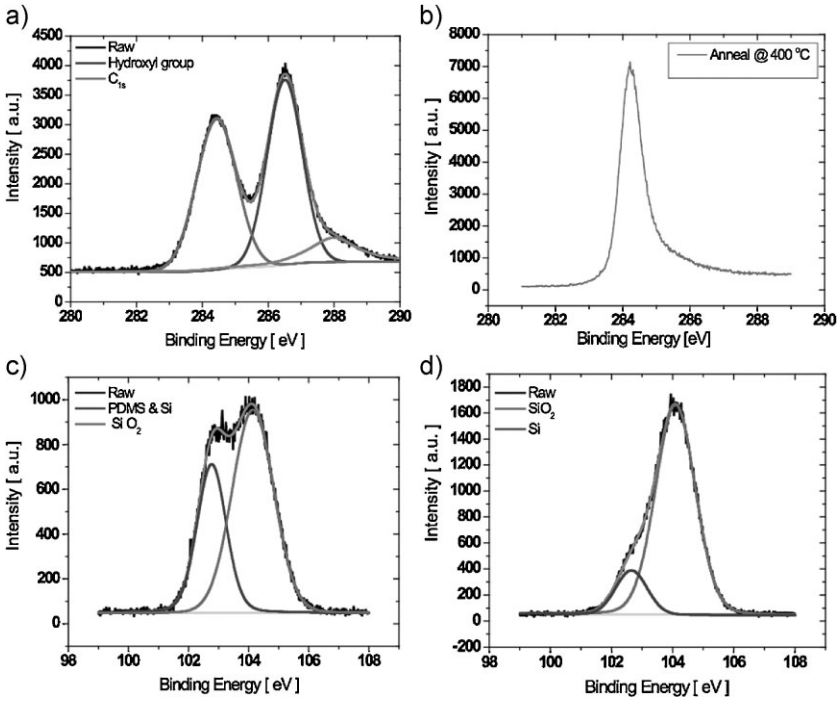

Figure 3. C 1s of graphite oxide: a) before annealing, b) after annealing. Si 2p spectra: c) before annealing, d) after annealing. The peak shifts of nearly 1 eV for Si and SiO_2 are attributed to a charging effect from the thick insulating oxide.

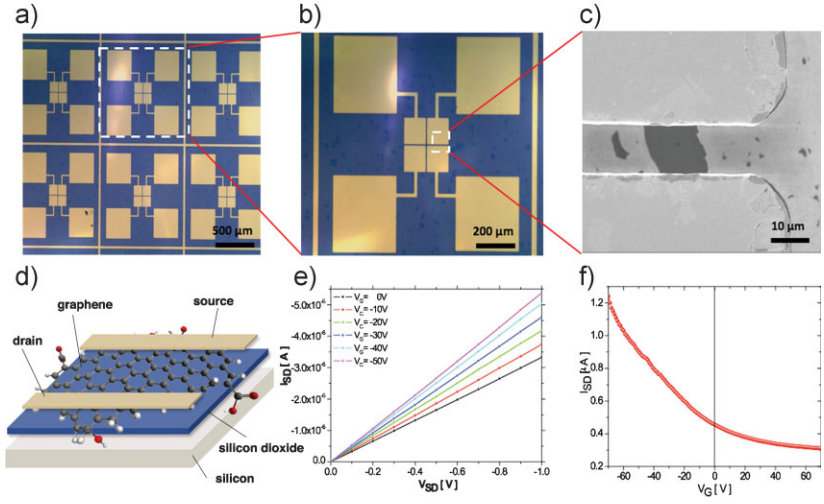

Figure 4. a,b) Optical images show the geometric layout of field effect devices. Gold electrodes are patterned via conventional photolithography to form top-contacts on the Si/SiO_2 substrate. c) An SEM image verifies a single sheet of graphene (dark region) bridging the electrodes (top and bottom). d) A diagram shows the structure of the fabricated devices. e) I_{SD}–V_{SD} measurements and f) I_{SD}–V_G transfer curves indicate current modulation under negative gate bias.

indicating complete removal of PDMS residue. XPS signals were recorded on other areas of the wafer after annealing, but showed no signs of dimethylsiloxane. This likely indicates that oligomers either volatilized in the high vacuum of the XPS chamber or decomposed beyond recognition. The shift of peaks identified as SiO_2 at 104.4 eV and PDMS at 102.6 eV is attributed to a charging effect by the thick insulating layer of SiO_2 (300 nm).[25] The carbon signal does not change before and after the process, an indication that annealing did not alter the deposited graphene. If anything, the heat treatment may increase the graphitization of single sheets, as has been indicated by other groups.[32]

Characterization of Single Sheets: The electrical properties of chemically converted graphene depositions were confirmed by the fabrication of field-effect devices. Briefly, gold electrodes were patterned via a conventional photolithographic lift-off process, with electrode separation lengths of 7 micrometers. Optical images of the fabricated devices are provided at 10× and 20× magnification in Figure 4a and b, respectively. We did not use any alignment techniques to predetermine the location of the electrodes. Instead, we patterned a large array (10×10) and relied on the uniformity of our deposition to produce working devices. After evaporation, SEM was used to identify single sheet devices as depicted in Figure 4c. Gate voltages were supplied via the Si substrate, providing I_{SD}–V_{SD} characteristics as depicted in Figure 4e. As shown in the figure, deposited graphene materials increased in conductivity under negative gating conditions, indicating p-type behavior. We attribute the lack of ambipolar effect to hole doping caused by residual oxygen functionalities. Figure 4f shows a transfer curve (I_{SD}–V_G) collected at a V_{SD} of 100 mV. These observations agree well with others of chemically converted graphene.[14]

Atomic force microscopy (AFM) was also used to confirm the edge step heights of graphene sheets. Figure 5 shows an AFM image collected in tapping mode and a corresponding line-scan, which indicates a step height of less than 1 nm. Although the theoretical thickness of pristine graphene is 0.34 nm, measurements rarely approach this number even in ultra-high vacuum settings.[13–15] In our case, AFM images were collected under ambient conditions, where adsorbed water and gas molecules typically result in step heights around 1 nm for both pristine and chemically converted graphene.[13–15]

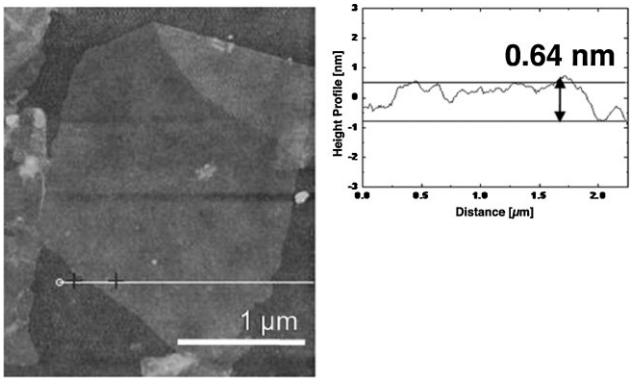

Figure 5. An AFM image (left) and the corresponding line-scan (right) confirm a step height of less than 1 nm, indicative of single sheet graphene.

Experimental

Preparation of Graphene Dispersions: We prepared graphite oxide (GO) from graphite powder via the Hummer's method [33]. Resultant dispersions were 2% w/v in water and diluted to 1 mg L^{-1} for use. GO was then filtered through a 0.22 micrometer alumina membrane in order to create a thin film, which we allowed to dry for 24 hours under ambient conditions and then carefully peeled from the membrane.

The GO film was matte black in color and physically robust. Elemental analysis was performed by ICP-Mass Lab, UCLA, CA. Elemental analysis of the GO product suggests that its atomic composition (wt %) is: C, 43.83%; O, 44.0%; N, 0%; residual value 9.6%. This yields a C:O:N ratio of: 4:3:0 with a C/O value of 1.33, an indicative of highly oxidized GO material. As for preparing a solution, a small piece of the GO film (≈1 mg) was transferred into a nitrogen filled dry box, and added to 1 mL of anhydrous hydrazine for reduction and dispersion. Upon contact, a gaseous product bubbled from the surface of the film, likely N_2 evolved during the reduction process. During this bubbling, the film was seen breaking down and hydrazine underwent a change from clear to a dark black color, indicating the dispersion of reduced graphite oxide. The hydrazine dispersions likely contained hydrazinium graphene (HG) due to the formation of a counter-ion pair during reduction [34]. After 24 hours of stirring, no residual film was observed. Elemental analysis of HG was performed by evaporating the solvent under streaming nitrogen, producing a dry, shiny black material that yielded a C:O:N ratio of approximately 8:1:1.5.

HG dispersions were stable and allowed to stir for up to several months in a covered vial before deposition. Further treatment of HG suspensions was carried out just before spin-coating, and differed according to the desired level of surface coverage. A Heraeus Labofuge 400 was used for centrifugation, which removed any aggregates prior to spin-coating. Sonication was carried out using a VWR model 250D sonicator set at level 9 for 10 min.

Preparation of Films: Si/SiO_2 substrates were cleaned in piranha solution and pre-treated for 2 minutes by an oxygen plasma in order to ensure good wetting by hydrazine. Substrates were transferred into the dry box and spin-coated within 15 minutes of this pre-treatment. After deposition, films were baked at 115 °C to remove residual hydrazine and then heated to 350 °C in order to remove hydrazinium ions. Elemental analysis carried out on the final material produced a C:O:N ratio of 12:1:0.7, confirming the removal of nitrogen-containing species.

Acknowledgements

M. J. A. and V. C. T. contributed equally to this work. We acknowledge the financial support from the National Science Foundation Grant DMR-0507294, its NSF-IGERT program (MJA), the Air Force Office of Scientific Research Grant FA95500710264 (YY), and the FCRP FENA center (RBK). Supporting Information is available online from Wiley InterScience or from the author.

Received: October 13, 2008
Published online: March 4, 2009

[1] K. S. Novoselov, A. K. Geim, S. V. Morozov, D. Jiang, Y. Zhang, S. V. Dubonos, I. V. Grigorieva, A. A. Firsov, *Science* **2004**, *306*, 666.
[2] V. P. Gusynin, S. G. Sharapov, *Phys. Rev. Lett.* **2005**, *95*, 146801.
[3] Y. Zhang, Y. W. Tan, H. L. Stormer, P. Kim, *Nature* **2005**, *438*, 201.
[4] K. S. Novoselov, E. McCann, S. V. Morozov, V. I. Fal'ko, M. I. Katsnelson, U. Zeitler, D. Jiang, F. Schedin, A. K. Geim, *Nat. Phys.* **2006**, *2*, 177.
[5] K. S. Novoselov, Z. Jiang, Y. Zhang, S. V. Morozov, H. L. Stormer, U. Zeitler, G. S. Boebinger, P. Kim, A. K. Geim, *Science* **2007**, *315*, 1379.
[6] K. S. Novoselov, A. K. Geim, S. V. Morozov, D. Jiang, M. I. Katsnelson, I. V. Grigorieva, S. V. Dubonos, A. A. Firsov, *Nature* **2005**, *438*, 197.

[7] C. Berger, Z. Song, T. Li, X. Li, A. Y. Ogbazghi, R. Feng, Z. Dai, A. N. Marchenkov, E. H. Conrad, P. N. First, W. A. de Heer, *J. Phys. Chem. B* **2004**, *108*, 19912.

[8] C. Berger, Z. Song, X. Li, X. Wu, N. Brown, C. Naud, D. Mayou, T. Li, J. Hass, A. N. Marchenkov, E. H. Conrad, P. N. First, W. A. de Heer, *Science* **2006**, *312*, 1191.

[9] L. M. Viculis, J. J. Mack, R. B. Kaner, *Science* **2003**, *299*, 1361.

[10] H. Shioyama, T. Akita, *Carbon* **2003**, *41*, 179.

[11] I. Jung, D. A. Dikin, R. D. Piner, R. S. Ruoff, *Nano Lett.* **2008**, *8*, 2483.

[12] S. Stankovich, D. A. Dikin, R. D. Piner, K. A. Kohlhaas, A. Kleinhammes, Y. Jia, Y. Wu, S. T. Nguyen, R. S. Ruoff, *Carbon* **2007**, *45*, 1558.

[13] C. Gomez-Navarro, R. T. Weitz, A. M. Bittner, M. Scolari, A. Mews, M. Burghrd, K. Kern, *Nano Lett.* **2007**, *7*, 3499.

[14] S. Gilje, S. Han, M. S. Wang, K. L. Wang, R. B. Kaner, *Nano Lett.* **2007**, *7*, 3394.

[15] C. Gómez-Navarro, R. Weitz, A. M. Bittner, M. Scolari, A. Mews, M. Burghard, K. Kern, *Nano Lett.* **2007**, *7*, 3499.

[16] V. C. Tung, M. J. Allen, Y. Yang, R. B. Kaner, *Nat. Nanotechnol.* **2009**, *4*, 25.

[17] M. L. Chabinyc, A. Salleo, Y. Wu, P. Liu, B. S. Ong, M. Heeney, I. McCulloch, *J. Am. Chem. Soc.* **2004**, *126*, 13928.

[18] A. C. Arias, S. E. Ready, R. Lujan, W. S. Wong, K. E. Paul, A. Salleo, M. L. Chabinyc, R. Apte, R. A. Street, Y. Wu, P. Liu, B. S. Ong, *Appl. Phys. Lett.* **2004**, *85*, 3304.

[19] T. Kawase, H. Sirringhaus, R. H. Friend, T. Shimoda, *Adv. Mater.* **2001**, *13*, 1601.

[20] M. Lefenfeld, G. Blanchet, J. Rogers, *Adv. Mater.* **2003**, *15*, 1188.

[21] M. L. Chabinyc, W. S. Wong, A. Salleo, E. P. Kateri, R. A. Street, *Appl. Phys. Lett.* **2002**, *81*, 4260.

[22] X. Liang, Z. Fu, S. Y. Chou, *Nano Lett.* **2007**, *7*, 3840.

[23] J.-H. Chen, M. Ishigami, C. Jang, D. R. Hines, M. S. Fuhrer, E. D. Williams, *Adv. Mater.* **2007**, *19*, 3623.

[24] S.-H. Hur, D.-Y. Khang, C. Kocabas, J. A. Rogers, *Appl. Phys. Lett.* **2004**, *85*, 5730.

[25] A. L. Briseno, M. Roberts, M. M. Ling, H. Moon, E. J. Nemanick, Z. Bao, *J. Am. Chem. Soc.* **2004**, *126*, 13928.

[26] K. Glasmastar, J. Gold, A. Andersson, D. S. Sutheland, B. Kasemo, *Langmuir* **2003**, *19*, 5475.

[27] X.-M. Li, M. Peter, J. Huskens, D. N. Reinhoudt, *Nano Lett.* **2003**, *3*, 1449.

[28] A. C. Ferrari, J. C. Meyer, V. Scardaci, C. Casiraghi, M. Lazzeri, F. Mauri, S. Piscanec, D. Jiang, K. S. Novoselov, S. Roth, A. K. Geim, *Phys. Rev. Lett.* **2006**, *97*, 87401.

[29] F. Tuinstra, J. L. Koenig, *J. Chem. Phys.* **1970**, *53*, 1126.

[30] A. Gupta, G. Chen, P. Joshi, S. Tadigadapa, P. C. Eklundi, *Nano Lett.* **2006**, *6*, 2667.

[31] D. Graf, F. Molitor, K. Ensslin, C. Stampfer, A. Jungen, C. Hierold, L. Wirtz, *Nano Lett.* **2007**, *7*, 238.

[32] H. Becerril, J. Mao, Z. Liu, R. Stoltenberg, Z. Bao, Y. Chen, *ACS Nano* **2008**, *2*, 463.

[33] W. S. Hummers, R. E. Offeman, *J. Am. Chem. Soc.* **1958**, *80*, 1339.

[34] B. D. Mitzi, M. Copel, S. J. Chey, *Adv. Mater.* **2005**, *17*, 1289.